



**HAL**  
open science

## Phenomenological modelling of light transmission through nanowires arrays

Junze Zhou, Loïc Le Cunff, Komla Nomenyo, Alexandre Vial, T. Pauporté,  
Gilles Lerondel

► **To cite this version:**

Junze Zhou, Loïc Le Cunff, Komla Nomenyo, Alexandre Vial, T. Pauporté, et al.. Phenomenological modelling of light transmission through nanowires arrays. *Thin Solid Films*, 2019, 675, pp.43-49. 10.1016/j.tsf.2019.01.054 . hal-02357502

**HAL Id: hal-02357502**

**<https://hal.science/hal-02357502>**

Submitted on 22 Oct 2021

**HAL** is a multi-disciplinary open access archive for the deposit and dissemination of scientific research documents, whether they are published or not. The documents may come from teaching and research institutions in France or abroad, or from public or private research centers.

L'archive ouverte pluridisciplinaire **HAL**, est destinée au dépôt et à la diffusion de documents scientifiques de niveau recherche, publiés ou non, émanant des établissements d'enseignement et de recherche français ou étrangers, des laboratoires publics ou privés.



Distributed under a Creative Commons Attribution - NonCommercial 4.0 International License

# Phenomenological modelling of light transmission through nanowires arrays

J. Zhou<sup>1\*</sup>, L. O. Le Cunff<sup>1</sup>, K. Nomenyo<sup>1</sup>, A. Vial<sup>1</sup>, T. Pauporté<sup>2</sup> and G. Lerondel<sup>1\*</sup>

<sup>1</sup>*Lumière, nanomatériaux, nanotechnologie (L2n), Institut Charles Delaunay, CNRS FRE 2019 (UMR 6281), Université de Technologie de Troyes, 12 rue Marie Curie, CS 42060, 10004 Troyes Cedex, France*

<sup>2</sup>*Chimie Paristech, PSL Research University, CNRS, Institut de Recherche de Chimie Paris (IRCP), 11 rue Pierre et Marie Curie, 75005 Paris, France*

*\*Corresponding authors*

A phenomenological model has been developed and discussed. The model is able to describe the experimentally measured light transmission of nanowires arrays. Two representative samples were studied in this report. A well aligned nanowires sample was first modelled by an effective layer model with surface roughness added. Then a slightly tilted nanowires sample with round top was phenomenologically modelled by a two layers model with a first top layer of an effective medium which includes a volume scattering contribution (Mie theory). Roughness and waviness are added to account for the nanowires small and large scale fluctuation in height. This phenomenological description was proven to be feasible by fitting experimental data. As a conclusion, light transmitted through randomly distributed nanowires can be explained by the combination of volume and surface scatterings using respectively Mie theory and rough Fresnel coefficients at the interfaces.

# 1. Introduction

One-dimensional semiconductor nanowires are of a great interest for a large number of electronic and photonic devices due to their physical properties coming from electronic or quantum confinement [1-4]. In particular, ZnO nanowires thin films are among the most promising materials, because of a large exciton binding energy (60 meV), a wide bandgap (3.37eV), a resistance to harsh environments as well as the existence of relatively easy nanofabrication methods like the catalyst-assisted vapor-liquid-solid growth method[5-6], chemical bath deposition (CBD) [7] or electrochemical deposition (ECD) [8, 9]. ZnO nanowires are attractive building blocks for many optoelectronic devices such as ultraviolet lasers [10, 11], gas sensors [12, 13], light emitting diodes [14, 15], and photodetectors [16, 17].

Many theoretical works that have aimed at calculating the transmission of nanowires thin films are based on numerical studies using the finite-difference time-domain method (FDTD) method [18-23]. FDTD appears as a straightforward method to simulate light interaction with nanowires, however, this approach is very time consuming and requires to know the exact geometry of the samples. As the solution grown nanowires are randomly distributed and usually tilted on the substrate, the exact geometry is almost impossible to assess. In this context, phenomenological modelling appears more appropriate to describe the optical properties of the arrays. As an examples, similar approach has already been applied to simulate the optical properties of Cu nanowires [24]. In this paper, we report on the phenomenological modelling of the light transmission of nanowires arrays through parameters coming from the fitting of the direct transmission of a ZnO nanowire array sample. A rather simple analytical model is developed to describe the optical response of the sample.

## 2. Theory and calculation

### 2.1. Transfer matrix method and rough Fresnel coefficients

The transmission of a multilayer system is readily calculated by the transfer matrix method [25]. In the matrix,  $A_i^\downarrow$  is the amplitude of the electromagnetic wave propagating in

the positive direction, which is the same direction as the incident light.  $A_i^\uparrow$  is the amplitude of the electromagnetic wave propagating in the negative direction. The Light amplitude in air  $A_0^\downarrow$  and  $A_0^\uparrow$  can be calculated in the following form by:

$$\begin{bmatrix} A_0^\downarrow \\ A_0^\uparrow \end{bmatrix} = M_1 L_1 M_2 L_2 \cdots M_i \begin{bmatrix} A_i^\downarrow \\ A_i^\uparrow \end{bmatrix} \quad (1)$$

where  $M_i$  is the transmission matrix at the flat interface between two media layers  $i - 1$  and  $i$  given by:

$$M_i = \frac{1}{t_{i-1,i}} \begin{bmatrix} 1 & r_{i-1,i} \\ r_{i-1,i} & 1 \end{bmatrix} \quad (2)$$

where  $t_{i-1,i}$  and  $r_{i-1,i}$  are respectively the Fresnel transmission and reflection coefficients of the interface between layers  $i - 1$  and  $i$ . The propagation matrix  $L_i$ , which relates the field amplitude in the top and bottom sides of the layer  $i$ , is given by:

$$L_i = \begin{bmatrix} e^{-j\beta_i} & 0 \\ 0 & e^{j\beta_i} \end{bmatrix} \quad (3)$$

where  $\beta_i$  is given by:

$$\beta_i = \frac{2\pi}{\lambda} d_i n_i \cos \theta_i \quad (4)$$

$\lambda$  is the wavelength of the incident field,  $d_i$  is the thickness of the  $i$ -th layer, and  $\theta_i$  is the incident angle at the interface between layers  $i - 1$  and  $i$ .

If we assume the field amplitudes in the bottom layer to be  $A_i^\downarrow = 1$  and  $A_i^\uparrow = 0$ , then the transmission of the multilayers structure can be expressed as:

$$T = \frac{n_i}{n_0} \left( \frac{1}{A_0^\downarrow} \right)^2 \quad (5)$$

To calculate the surface scattering between the interfaces of the rough layers, the rough Fresnel coefficients equations were applied. G. Léron del and R. Romestain [26] have derived a second-order approximation solution, and the simplified reflection coefficients  $r_{i-1,i}$  and transmission coefficients  $t_{i-1,i}$  of a rough layer have been given in the special case of small scattering angles:

$$r_{i-1,i} = \frac{k_{i-1} - k_i}{k_{i-1} + k_i} \{1 - 4k_{i-1}^2 \xi_i^2\} \quad (6)$$

$$t_{i-1,i} = \frac{2k_{i-1}}{k_{i-1} + k_i} [1 - (k_{i-1} - k_i)^2 \xi_i^2] \quad (7)$$

where  $k_{i-1}$  and  $k_i$  are the wave factors of the incident wave and transmitted wave at the rough surface of the layer  $i$ , and  $\xi_i$  is the amplitude of the sine profile roughness.

The transfer coefficients for the amplitude of forward and backward waves  $A_{i-1}$  and  $A'_{i-1}$  in the medium  $i - 1$  as a function of the amplitude  $A_i$  and  $A'_i$  in the medium  $i$  are obtained:

$$\begin{bmatrix} A_{i-1}^\downarrow \\ A'_{i-1}^\uparrow \end{bmatrix} = M_i \begin{bmatrix} A_i^\downarrow \\ A'_i^\uparrow \end{bmatrix} \quad (8)$$

Then the transmission matrix  $M_i$  that links the amplitude of the waves on the two sides of the rough interfaces is given by:

$$M_i = \begin{bmatrix} a_i & b_i \\ c_i & d_i \end{bmatrix} \quad (9)$$

with:

$$a_i = \frac{k_{i-1} + k_i}{2k_{i-1}} [1 + (k_{i-1} - k_i)^2 \xi_i^2] \quad (10)$$

$$b_i = \frac{k_{i-1} - k_i}{2k_{i-1}} \{1 + (k_{i-1} - k_i)^2 - 4k_{i-1}^2 \xi_i^2\} \quad (11)$$

$$c_i = \frac{k_{i-1} - k_i}{2k_{i-1}} [1 + [(k_{i-1} - k_i)^2 - 4k_{i-1}^2] \xi_i^2] \quad (12)$$

$$d_i = \frac{k_{i-1} + k_i}{2k_{i-1}} \{1 + 3(k_{i-1} - k_i)^2 \xi_i^2\} \quad (13)$$

## 2.2. Effective medium theory (EMT)

EMTs have been developed to calculate the effective permittivity of a composite material system. In our modelling, we selected Maxwell-Garnett model [27]. To simulate the porous properties of an effective layer composed of Mie scattering nanosphere and air. The effective permittivity  $\varepsilon_1$  of this layer can be derived from the following equation:

$$\frac{\varepsilon_1 - \varepsilon_{air}}{\varepsilon_1 + 2\varepsilon_{air}} = f_1 \frac{\varepsilon_{sp} - \varepsilon_{air}}{\varepsilon_{sp} + 2\varepsilon_{air}} \quad (14)$$

where  $f_1$  is the density of the nanospheres in the effective layer,  $\varepsilon_{air}$  is the permittivity of the air and  $\varepsilon_{sp}$  is the permittivity of the nanospheres, which will be introduced in the following section.

As for another effective layer, which are composed of nonspherical material and air. We selected the Landau Lifshitz/Looyenga model [28] [29] as the effective medium model. The effective permittivity  $\varepsilon_2$  can be deduced from the following equation:

$$\sqrt[3]{\varepsilon_2} = f_2 \sqrt[3]{\varepsilon_n} + (1 - f_2) \sqrt[3]{\varepsilon_{air}} \quad (15)$$

While  $f_2$  and  $\varepsilon_n$  are the volume fraction and permittivity of the component n.

### 2.3. Effective extinction coefficient of a homogenous nanosphere slab

Mie theory was applied to calculate effective extinction coefficient of a homogenous nanosphere slab [30]. The volume attenuation coefficient is given by:

$$\alpha = \frac{C_{ext}}{v} \quad (16)$$

while  $C_{ext}$  is the extinction cross-section of nanosphere and  $v$  is the volume of nanosphere. From equation (16), one can easily retrieve the imaginary part of the refractive index that accounts for the extinction (absorption and scattering):

$$k = \frac{C_{ext} \lambda}{4v\pi} \quad (17)$$

The refractive index of a homogenous nanosphere slab with Mie contribution can be expressed as:

$$\tilde{n} = n + \frac{C_{ext} \lambda}{4v\pi} i \quad (18)$$

we consider here that the real part is not affected as we are dealing with a homogenous slab.

### 2.4. The combined model

In this work, we have developed a combined model to phenomenologically model randomly distributed nanowires thin film. Figure 1 shows the sketches of the sample (left) and the model (right). We modeled the nanowire by two effective

medium layers with the first top layer includes Mie contribution accounting for the light scattering by the top of the nanowires. Roughness and waviness are added to account for the nanowires small and large scale fluctuations. Parameters have been chosen to be directly linked to the real geometry of the sample. In the phenomenological model, the average diameter of the nanowires  $d$  corresponds to the diameter of sphere, the average height of nanowires  $e$  corresponds to the sum of the first and second layer thicknesses,  $e_m + d$ , the small scale height fluctuations  $\zeta$  corresponds to the roughness  $\zeta_m$  and finally the large scale height fluctuations  $w$  corresponds to the waviness  $\sigma$ .

By applying equation (1) we can calculate the field amplitude in air (see the appendix for the matrix configuration):

$$\begin{bmatrix} A_0^\downarrow \\ A_0^\uparrow \end{bmatrix} = M_1 L_1 M_2 L_2 M_3 L_3 M_4 \dots M_n L_n M_s \begin{bmatrix} A_s^\downarrow \\ A_s^\uparrow \end{bmatrix} \quad (19)$$

while  $M_1, M_3$  are transmission matrices at the two rough interface 1 and 3, and  $M_4, M_n$  and  $M_s$  the transmission matrix at the interface 4, n and s. Then the equation (19) can be given by:

$$\begin{bmatrix} A_0^\downarrow \\ A_0^\uparrow \end{bmatrix} = \begin{bmatrix} a_1 & b_1 \\ c_1 & d_1 \end{bmatrix} \begin{bmatrix} e^{-j\beta_1} & 0 \\ 0 & e^{j\beta_1} \end{bmatrix} \frac{1}{t_{12}} \begin{bmatrix} 1 & r_{12} \\ r_{12} & 1 \end{bmatrix} \begin{bmatrix} e^{-j\beta_2} & 0 \\ 0 & e^{j\beta_2} \end{bmatrix} \begin{bmatrix} a_3 & b_3 \\ c_3 & d_3 \end{bmatrix} \begin{bmatrix} e^{-j\beta_3} & 0 \\ 0 & e^{j\beta_3} \end{bmatrix} \dots M_s \begin{bmatrix} A_s^\downarrow \\ A_s^\uparrow \end{bmatrix} \quad (20)$$

The transmission is given by:

$$T_m = \frac{n_s}{n_0} \left( \frac{1}{A_0^\downarrow} \right)^2 \quad (21)$$

The multilayers transmission is modified by the bottom reflection of the glass, which is simply the Fresnel reflection between glass and air, and then the transmission is given by:

$$T_s = T_m (1 - R_s) \quad (22)$$

As for the thickness and diameter fluctuations called here thickness and diameter waviness respectively we took a simple weighting function by considering the fraction as 1:2:5:2:1, which come from the Gaussian-like distribution of the thickness. This method has already been used in the case of porous silicon film [31] and Gaussian distribution of diameters has been observed in the CBD growth nanowires as well[7]. Then the final transmission of the combined model is expressed as:

$$T = \sum_{w=-2}^2 C_w \sum_{v=-2}^2 C_v \sum_{u=-2}^2 C_u T_s(d_u + u\sigma_u, d_v + v\sigma_v, d_w + w\sigma_w) \quad (23)$$

where  $u, v, w$  represent the coating layer of the substrate, the effective layers and the nanospheres,  $d$  is the thickness (diameter for the nanospheres),  $\sigma$  is the waviness (dispersion for the nanospheres),  $C$  is the weighting value:  $C_{-2} = \frac{1}{11}$ ,  $C_{-1} = \frac{2}{11}$ ,  $C_0 = \frac{5}{11}$ ,  $C_1 = \frac{2}{11}$ ,  $C_2 = \frac{1}{11}$ .

The reflection of the combined model is calculated in the same way:

$$R_s = \left(\frac{A_0^\uparrow}{A_0^\downarrow}\right)^2 \quad (24)$$

The final reflection of the combined model is given by:

$$R = \sum_{w=-2}^2 C_w \sum_{v=-2}^2 C_v \sum_{u=-2}^2 C_u R_s(d_u + u\sigma_u, d_v + v\sigma_v, d_w + w\sigma_w) \quad (25)$$

The signal attenuation (absorption and scattering) then is expressed as:

$$A = 1 - T - R \quad (26)$$

### 3. Experimental details

The first ZnO nanowires thin film sample studied in this paper was prepared by CBD method. 0.035M zinc acetate was dissolved in 750 mL of deionized water. 9ml of ammonium hydroxide was added to this solution. The ZnO seed layer pre-coated quartz substrate was immersed in this solution for one hour at 87°C (details of the deposition technique can be found in the literature [7]). The second ZnO nanowires sample was obtained by ECD method, in the following condition:  $C[\text{Zn}(\text{ClO}_4)] = 0.2 \text{ mM}$ ,  $Q = 23.81 \text{ C.cm}^{-2}$  and molecular oxygen bubbling (details of the deposition technique and conditions can be found in the literature [8, 9]), The sample was grown on a FTO thin film coated glass substrate, the thickness of the FTO layer was about 1  $\mu\text{m}$ .

The morphologies of the samples were characterized by the Field-emission Scanning Electron Microscope (FEG-SEM Hitachi SU8030 at 10 kV) and the Atomic Force Microscope (AFM 5100 Agilent). The optical transmission curves of the ZnO nanowires samples were measured using a UV-VIS-NIR spectrophotometer (Cary 100) with a spot size



of  $2 \text{ mm} \times 5 \text{ mm}$ , which is much bigger than the size of the nanowires and the distance between them. In this regard, the studied nanostructure samples in this work have large scale uniformity compared to the spot size. Moreover large scale homogeneity has been assessed by measuring the transmission on different spots of the sample.

## **4. Results**

### **4.1. Morphology and Transmission curves**

The SEM image (inset of Figure 2 (a)) shows that the nanowires of sample 1 were relatively well aligned and perpendicular to the substrate. They were closely compact, with a diameter and length in the order of 50 nm and 810 nm respectively. Figure 2 (a) displays the transmission curve of sample 1. This curve shows some fringes in the visible range and a sharp decrease of the transmission at shorter wavelengths, which is attributable to near band edge absorption. Those features are typical of the transmission of a ZnO thin film.

The inset of Figure 2 (b) shows a cross-section of sample 2. The diameter and length of the nanowires were in the order of 200 nm and 450 nm, and the nanowires were more tilted compared to the sample 1. The angle is however smaller than  $30^\circ$  with respect to the substrate normal vector. Figure 2 (b) shows the transmission curves of the substrate alone (FTO-coated glass) and sample 2. The transmission curve of the substrate has the similar features as the one of sample 1. For the full sample, the curve shows almost no transmission below 375 nm, which is due to the absorption by the ZnO. The transmission has a fairly constant value over the range of 400 to 470nm and then increases monotonically at longer wavelengths.

### **4.2. The rough layer model**

The applicability of the rough layer model was first verified by respectively modelling the optical transmission curves of sample 1 and of the FTO substrate used for sample 2.

As described in the previous part, the nanowires of sample 1 are very compact and have small diameter, a rough porous thin film model (inset drawing of Figure 3) is applied to fit the transmission curve. Figure 3 shows the calculated curves with different parameters and the experimental data. The best fitting curve was calculated by the following parameters: The

thickness of the ZnO thin films is 810 nm with a waviness of 30 nm. The surface roughness is equal to 18 nm. As for the modeling on the porous properties of the thin film, we selected the Landau-Lifshitz/Looyenga model as the effective medium model, with a ZnO volume fraction of 73%, which is fairly comparable to the density of the close packed ZnO nanowires. The good fitting in Figure 3 indicates that the light scattering of sample 1 can be explained by small angle scattering only due to surface roughness. The effective medium theory works well to simulate the nanowires thin film as a porous thin film, since the diameters of the nanowires are much smaller than the light wavelength.

Then we simulate the transmission curve of the FTO substrate of the second sample with a rough thin film model. We need first to define the parameters of the substrate, including the thickness, roughness and waviness amplitudes and the refractive index of the FTO layer. Figure 4 (b) and Figure 4 (c) show the SEM and atomic force microscope images of the FTO layer. The roughness root mean square of the FTO layer can be obtained from the AFM image which is equal to 29.5 nm. The insert of Figure 4 (d) shows the model used to calculate the transmission curve of the substrate. With the known roughness amplitude, the other parameters in the calculation are obtained by fitting the measured transmission curve.

Figure 4(a) shows the calculated transmission curves of a flat substrate and a rough substrate. The transmission of the rough substrate is lower and shows less contrast in the fringes, which is due to the scattering by the surface roughness. The simulated curve of the rough substrate fits better with the experimental data.

Nevertheless, to well account for the experimental data, a further decrease of the fringes contrast is needed. Waviness was added. The waviness was accounted by averaging the transmission for five different thicknesses, 1010 nm,  $1010 \pm 20$  nm, and  $1010 \pm 40$  nm with a respective weight of 5, 3, 3, 1, 1. Compared to the case without waviness in Figure 4(a), Figure 4 (d) shows that the simulated transmission curve of a rough substrate with thickness fluctuation has less contrast in the fringes, and fit very well the experimental data.

The inset in Figure 4(a) shows the refractive index deduced from the fitting by the gradient descent optimization method, which is comparable to the refractive index for the FTO thin film in the literature [32]. We used the same optimization method to optimize the thickness, waviness, the amplitude of the roughness and the refractive index of FTO at the same time. The optimized values are as follows: the thickness of the rough FTO layer  $d_{FTO} =$

1010 nm, the roughness amplitude  $\xi_{FTO} = 29.5$  nm and the thickness waviness amplitude,  $\sigma_{FTO}$  equals to 20 nm.

### 4.3. The combined model

To achieve the best fitting between the calculation from the combined model and measured curve, we first assess the contributions of the different parameters. Figure 5 (a) shows the calculated optical transmission curves of three simple models. The first curve is calculated from the FTO coated substrate plus two effective ZnO layers. For the top layer, the thickness  $d = 220$  nm and density  $f_1=58\%$ , and for the second layer, the thickness is  $e_m = 480$  nm and the density is  $f_1=70\%$ . Referring to the transmission curve of the FTO substrate, this calculated curve has more interference fringes because of the larger thickness. There are obvious disturbances of the fringes from 420 nm to 500 nm, which is due to the difference in the effective refractive index of the two layers. The dotted curve of Figure 5 (a) is the transmission of the substrate plus two ZnO effective layer with roughness  $\xi_m=48$  nm in the top layer and total waviness  $\sigma= 120$ nm. Compared to the case without roughness and waviness, this curve has lower transmission and the contrast of the fringes is much less. Both of the two curves have no transmission in UV ranges because of the absorption of the ZnO layers. The third curve is the transmission calculated for the substrate plus an effective layer including Mie contribution which has the equal thickness and diameter of  $d = 220$  nm, density of sphere  $f_1=58\%$  estimated from the ratio between ZnO and air from the SEM image (inset of Figure 1(b)), dispersion of the diameter  $\sigma_{sp}=7$ nm. This curve shows that a dip at around 500 nm can be explained by Mie resonance that will induce a drop in the transmitted intensity as shown in the measured transmission of sample 2.

The inset of Figure 5(b) shows the combined model which is composed of the substrate, an effective ZnO layer and a nanosphere layer. The simulated curve is calculated based on the following parameters: the diameter of nanospheres  $d = 220$  nm and a size dispersion  $\sigma_{sp}$  equals to 7 nm, the thickness of the sphere layer and the ZnO effective layer are 220 nm and 480 nm respectively, the top surface roughness  $\xi_{ZnO}=48$  nm and the waviness amplitude,  $\sigma_{effective\ layers} = 140$  nm, which is around 20% of the total thickness. This optimized curve is the one that agrees the most with the measurement.

## 5. Discussion

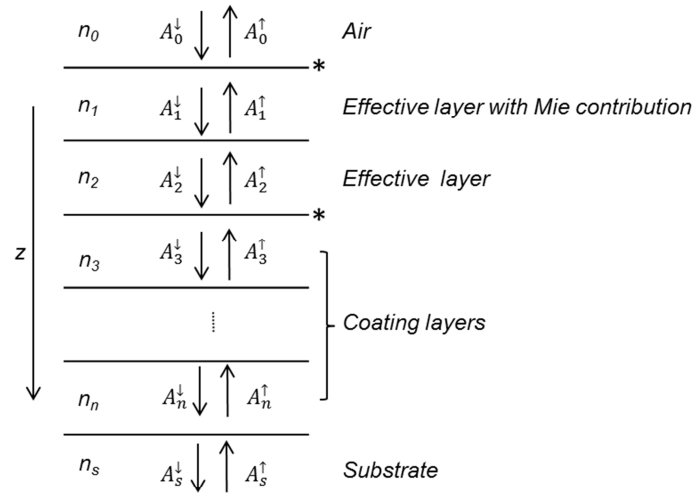
The transmission of ZnO nanowires is phenomenologically modelled by the combined model. In our model, the nanospheres are used to simplify the volume shape of the nanowires, while the roughness simplifies the top profile of the nanowires. The volume scattering and surface scattering effects are considered as the main factors for light scattering in the nanowires array. In addition, we add a ZnO thin film layer on the FTO layer to absorb the transmitted UV light through the first top layer. Furthermore, the waviness, thicknesses, and diameters that are applied in the model lead to a remarkable fit for the fringes contrast in the transmission curves. The goal behind the use of the simplified model is to explain that light interaction within the rather complicated sample can be simplified and considered as the combination of Mie and rough surface scatterings.

As for the phenomenological description, it is worth comparing the parameters of the combined model to the parameter of the nanowires in the real case. In the combined model, the combined structure including the slab of nanospheres, the rough and wavy ZnO layer is aiming at modelling the light interaction in the nanowires arrays. As shown in Table 1 comparing the measured and retrieved parameters, we find that the thickness of the combined structure (the layer of ZnO nanospheres plus the ZnO layer) is comparable to the length of the nanowires and that the diameter of the nanospheres (about 220 nm) matches the diameter of the nanowires as well. This very good agreement between measured and retrieved parameters confirms the veracity of the combined model proposed here. As the model i.e. generic model relies on three opto-geometrical parameters, the length and the diameter of the nanowires and their refractive index. The difference in height is accounted by the roughness parameter whereas the potential light scattering induced by the structures themselves is accounted by the Mie-theory. This phenomenological model can be easily applied to any other material based nanowire films which allows for a simple physical description of light interaction within nanowire arrays based thin films.

The main limitation lies in the fact that the description does not account for anisotropic diffractive structures. This will be a limitation for describing nanowires laying on a substrate which is here out of the scope of a thin film description. This model intends to described nanowire based thin films with the wires mainly oriented perpendicular to the substrates which is from far the most current case whatever the chemical or physical growth techniques excluding transfer techniques.

In summary, we have proposed a 1D matrix based phenomenological model to describe the transmission of randomly distributed nanowires arrays. The model relies on Mie scattering, interface roughness, and waviness. The simulations on the CBD grown nanowires sample and the FTO substrate firstly verified the applicability of the rough layer model. Then using the combined model, we have modelled light transmission of randomly distributed ECD growth ZnO nanowire array samples. Parameters determined from the fit are in a very good agreement with the experimental ones. Such a systematic study could potentially be used to predict the optical properties of any kind of nanowire samples and thus allowing for optimizing the structure features, by controlling the growth conditions on specific substrates.

## Appendix



\* Rough interface

## Acknowledgements

Authors would like to thank the Nano'mat platform for the use of characterization equipment. One the author, J. Z. would like to thank the Chinese Scholar Council for his Ph.D. fellowship.

## Notes and references

- [1] J. Hu, T.W. Odom, C.M. Lieber, Chemistry and physics in one dimension: synthesis and properties of nanowires and nanotubes, *Accounts of chemical research*, 32 (1999) 435-445.
- [2] Y. Wu, H. Yan, M. Huang, B. Messer, J. H. Song and P. Yang, Inorganic Semoconductor nanowires: rational growth, assembly, and novel properties, *Chemistry–A European Journal*, 8 (2002) 1260-1268.
- [3] X. Duan, Y. Huang, Y. Cui, J. Wang and C. M. Lieber, Indium phosphide nanowires as building blocks for nanoscale electronic and optoelectronic devices, *Nature*, 409 (2001), 66-69.
- [4] S. A. Mann and E. C. Garnett, Extreme light absorption in thin film semiconductor films wrapped around around metal nanowires *Nano letters*, 13 (2013) 3173-3178.
- [5] Z.L. Wang, Nanostructures of zinc oxide, *Materials today*, 7 (2004) 26-33.
- [6] Y. Kong, D. Yu, B. Zhang, W. Fang, S. Feng, Ultraviolet-emitting ZnO nanowires synthesized by a physical vapor deposition approach, *Applied Physics Letters*, 78 (2001) 407-409.
- [7] A. Gokarna, R. Parize, H. Kadiri, K. Nomenyo, G. Patriarche, P. Miska, G. Lerondel, Highly crystalline urchin-like structures made of ultra-thin zinc oxide nanowires, *RSC Advances*, 4 (2014) 47234-47239.
- [8] T. Pauporté, E. Jouanno, F. Pellé, B. Viana, P. Aschehoug, Key growth parameters for the electrodeposition of ZnO films with an intense UV-light emission at room temperature, *The Journal of Physical Chemistry C*, 113 (2009) 10422-10431.
- [9] O. Lupan, V. Guérin, I. Tiginyanu, V. Ursaki, L. Chow, H. Heinrich, T. Pauporté, Well-aligned arrays of vertically oriented ZnO nanowires electrodeposited on ITO-coated glass and their integration in dye sensitized solar cells, *Journal of Photochemistry and Photobiology A: Chemistry*, 211 (2010) 65-73.
- [10] S. Chu, G. Wang, W. Zhou, Y. Lin, L. Chernyak, J. Zhao, J. Kong, L. Li, J. Ren, J. Liu, Electrically pumped waveguide lasing from ZnO nanowires, *Nature nanotechnology*, 6 (2011) 506-510.
- [11] M.H. Huang, S. Mao, H. Feick, H. Yan, Y. Wu, H. Kind, E. Weber, R. Russo, P. Yang, Room-temperature ultraviolet nanowire nanolasers, *science*, 292 (2001) 1897-1899.

- [12] R. Aad, V. Simic, L. Le Cunff, L. Rocha, V. Sallet, C. Sartel, A. Lusson, C. Couteau, G. Lerondel, ZnO nanowires as effective luminescent sensing materials for nitroaromatic derivatives, *Nanoscale*, 5 (2013) 9176-9180.
- [13] J. Xu, J. Han, Y. Zhang, Y.a. Sun, B. Xie, Studies on alcohol sensing mechanism of ZnO based gas sensors, *Sensors and Actuators B: Chemical*, 132 (2008) 334-339.
- [14] J.H. Na, M. Kitamura, M. Arita, Y. Arakawa, Hybrid pn junction light-emitting diodes based on sputtered ZnO and organic semiconductors, *Applied Physics Letters*, 95 (2009).
- [15] H. Jeong, D.J. Park, H.S. Lee, Y.H. Ko, J.S. Yu, S.-B. Choi, D.-S. Lee, E.-K. Suh, M.S. Jeong, Light-extraction enhancement of a GaN-based LED covered with ZnO nanorod arrays, *Nanoscale*, 6 (2014) 4371-4378.
- [16] C.-Y. Lu, S.-J. Chang, S.-P. Chang, C.-T. Lee, C.-F. Kuo, H.-M. Chang, Y.-Z. Chiou, C.-L. Hsu, I. Chen, Ultraviolet photodetectors with ZnO nanowires prepared on ZnO: Ga/glass templates, *Applied Physics Letters*, 89 (2006) 15310-15311.
- [17] C. Soci, A. Zhang, B. Xiang, S.A. Dayeh, D. Aplin, J. Park, X. Bao, Y.-H. Lo, D. Wang, ZnO nanowire UV photodetectors with high internal gain, *Nano letters*, 7 (2007) 1003-1009.
- [18] C. Lundgren, R. Lopez, J. Redwing, K. Melde, FDTD modeling of solar energy absorption in silicon branched nanowires, *Optics express*, 21 (2013) A392-A400.
- [19] A.F. Oskooi, D. Roundy, M. Ibanescu, P. Bermel, J.D. Joannopoulos, S.G. Johnson, MEEP: A flexible free-software package for electromagnetic simulations by the FDTD method, *Computer Physics Communications*, 181 (2010) 687-702.
- [20] K. Seo, M. Wober, P. Steinvurzel, E. Schonbrun, Y. Dan, T. Ellenbogen, K.B. Crozier, Multicolored vertical silicon nanowires, *Nano letters*, 11 (2011) 1851-1856.
- [21] J. van de Groep, D. Gupta, M.A. Verschuuren, M. M. Wienk, R.A.J. Janssen, A. Polman, Large-area soft-imprinted nanowire networks as light trapping transparent conductors, *Scientific Reports*, 5 (2015) 11414.
- [22] K. Bae, G. Kang, S.K. Cho, W. Park, K. Kim, W.J. Padilla, Flexible thin-film black gold membranes with ultrabroadband plasmonic nanofocusing for efficient solar vapour generation, *Nature Communications*, 6 (2015) 10103.
- [23] G.K. Dalapati, A.K. Kushwaha, M. Sharma, V. Suresh, S. Shannigrahi, S. Zhuk, S. Masudy-Panah, Transparent heat regulating (THR) materials and coatings for energy saving window applications: Impact of materials design, micro-structural,



- and interface quality on the THR performance, *Progress in Materials Science*, 95 (2018) 42-131.
- [24] K. Locharoenrat, H. Sano, G. Mizutani, Phenomenological studies of optical properties of Cu nanowires, *Science and Technology of Advanced Materials*, 8 (2007) 277-281.
- [25] C.C. Katsidis, D.I. Siapkas, General transfer-matrix method for optical multilayer systems with coherent, partially coherent, and incoherent interference, *Appl. Opt.*, 41 (2002) 3978-3987.
- [26] G. Lérondel, R. Romestain, Fresnel coefficients of a rough interface, *Applied Physics Letters*, 74 (1999) 2740-2742.
- [27] J. C. Maxwell-Garebett, Colours in metal glasses and in metallic films. *Philos. Trans. Royal Soc. London A* 203 (1904) 385-420. DOI: 10.1098/rsta.1904.0024.
- [28] L. Landau and E. Lifshitz, *Electrodynamics of continuous media*, vol. 8 of course of *Theoretical Physics*, Pergamon Press, New York, 1982, 2nd ed.
- [29] H. Looyenga, Dielectric constants of heterogeneous mixtures, *Physica*, 31 (1965) 401-406.
- [30] C. F. Bohren and D. R. Huffman, *Absorption and scattering of light by small particles*, John Wiley & Sons 2008, pp. 80-81.
- [31] G. Lérondel, R. Romestain and S. Barret, Roughness of the porous silicon dissolution interface, *Journal of Applied Physics*, 81 (1997), 6171-6178.
- [32] J.M. Ball, M.M. Lee, A. Hey, H.J. Snaith, Low-temperature processed meso-structured to thin-film perovskite solar cells, *Energy & Environmental Science*, 6 (2013) 1739-1743.

## Figure and table captions

Fig.1. Phenomenological modelling of nanowires thin film: Sketches of the sample (left) and the used model (right). The model is mainly composed of a rough nanosphere layer with an effective medium refractive index  $n_{eff1}$  that includes light scattering contribution and a second layer of refractive index  $n_{eff2}$  to account for the porosity. The two layers model can be combined with any multilayer system such as coated transparent substrate including TCO coated glass. In the phenomenological modelling: The average diameter of the nanowires  $d$  corresponds to the diameter of the sphere; The average height of the nanowires  $e$  corresponds to the sum of the layer 1 and 2 thicknesses  $e_m + d$ ; The small scale height fluctuations  $\zeta$  corresponds to the roughness  $\zeta_m$ ; The large scale height fluctuations  $w$  corresponds to the waviness  $\sigma$ .

Fig.2. Optical transmission of typical nanowires samples: vertically aligned nanowires with flat top surface and tilted nanowires with round top. (a) Transmission curve of the CBD growth ZnO nanowires prepared on quartz substrate. (b) Transmission curves of the FTO coated glass substrate and the ECD growth ZnO nanowire arrays sample. The inserted images are respectively SEM images of the corresponding samples with respective scale bar.

Fig.3. Experimental and corresponding theoretical transmission curves of the ZnO sample 1 using the rough surface model (cf.inset) including waviness as represented by the dotted line.

Fig.4. Parameters assessment: (a) Calculated optical transmission curves of the flat substrate model, the rough substrate model and the experimental data. The inset represents is the refractive index (real and imaginary) of FTO, the  $x$  axis is the same as the one for the transmission curve. (b) SEM image of the FTO. (c) AFM image of the FTO layer surface. (d) Transmission curves of the rough surface model (cf. inset) with thickness waviness of the FTO thin films as to compare with the experimental data.

Fig.5. Combined model fitting: (a) Calculated optical transmission curves for the three models: FTO coated substrate plus two effective ZnO layers, FTO layer plus two ZnO effective medium layers with roughness and waviness applied, FTO layer plus a nanosphere layer. The arrows indicate the drop of transmission in the UV and visible range which are respectively the ZnO absorption and light scattering by the nanowires top part. (b) Transmission curve calculated by the combined model (inset image) and corresponding experimental data.

Table 1. Comparison between the measured parameters and the retrieved parameters from the combined model.

Fig.1. Phenomenological modelling of nanowires thin film: Sketches of the sample (left) and the used model (right). The model is mainly composed of a rough nanosphere layer with an effective medium refractive index  $n_{eff1}$  that includes light scattering contribution and a second layer of refractive index  $n_{eff2}$  to account for the porosity. The two layers model can be combined with any multilayer system such as coated transparent substrate including TCO coated glass. In the phenomenological modelling: The average diameter of the nanowires  $d$  corresponds to the diameter of the sphere; The average height of the nanowires  $e$  corresponds to the sum of the layer 1 and 2 thicknesses  $e_m + d$ ; The small scale height fluctuations  $\zeta$  corresponds to the roughness  $\zeta_m$ ; The large scale height fluctuations  $w$  corresponds to the waviness  $\sigma$ .

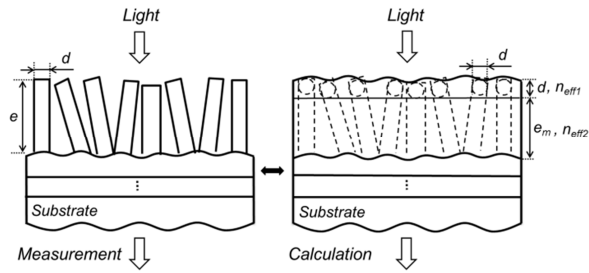


Fig.2. Optical transmission of typical nanowires samples: vertically aligned nanowires with flat top surface and tilted nanowires with round top. (a) Transmission curve of the CBD growth ZnO nanowires prepared on quartz substrate. (b) Transmission curves of the FTO coated glass substrate and the ECD growth ZnO nanowire arrays sample. The inserted images are respectively SEM images of the corresponding samples with respective scale bar.

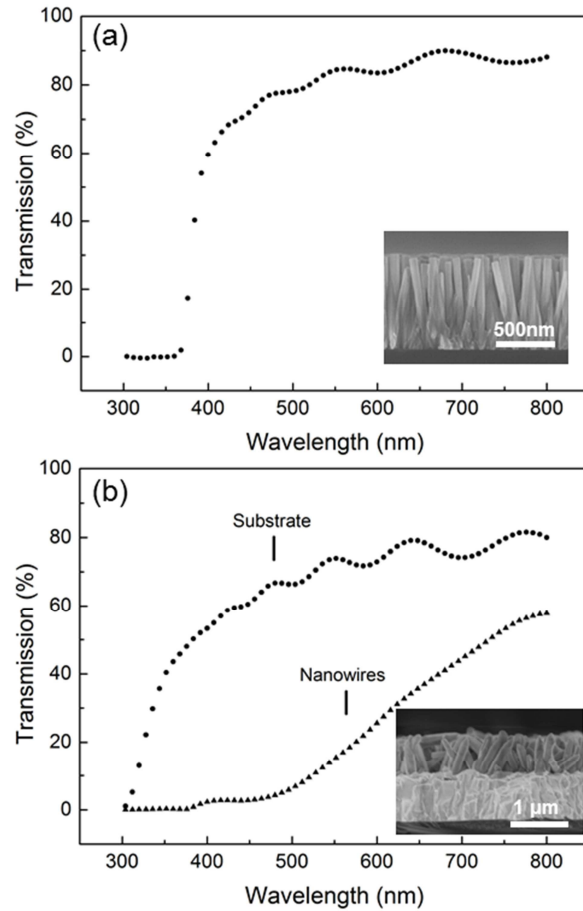


Fig.3. Experimental and corresponding theoretical transmission curves of the ZnO sample 1 using the rough surface model (cf.inset) including waviness as represented by the dotted line.

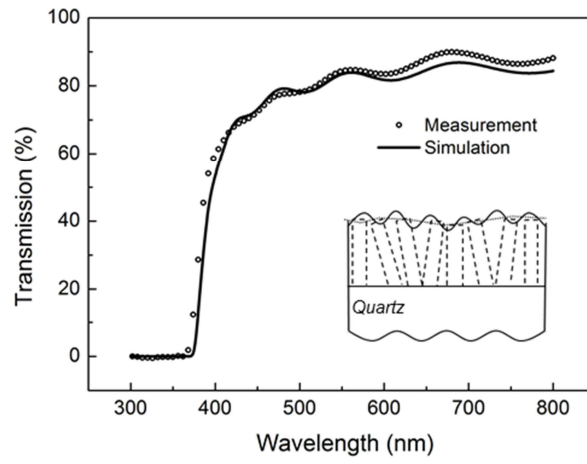


Fig.4. Parameters assessment: (a) Calculated optical transmission curves of the flat substrate model, the rough substrate model and the experimental data. The inset represents is the refractive index (real and imaginary) of FTO, the  $x$  axis is the same as the one for the transmission curve. (b) SEM image of the FTO. (c) AFM image of the FTO layer surface. (d) Transmission curves of the rough surface model (cf. inset) with thickness waviness of the FTO thin films as to compare with the experimental data.

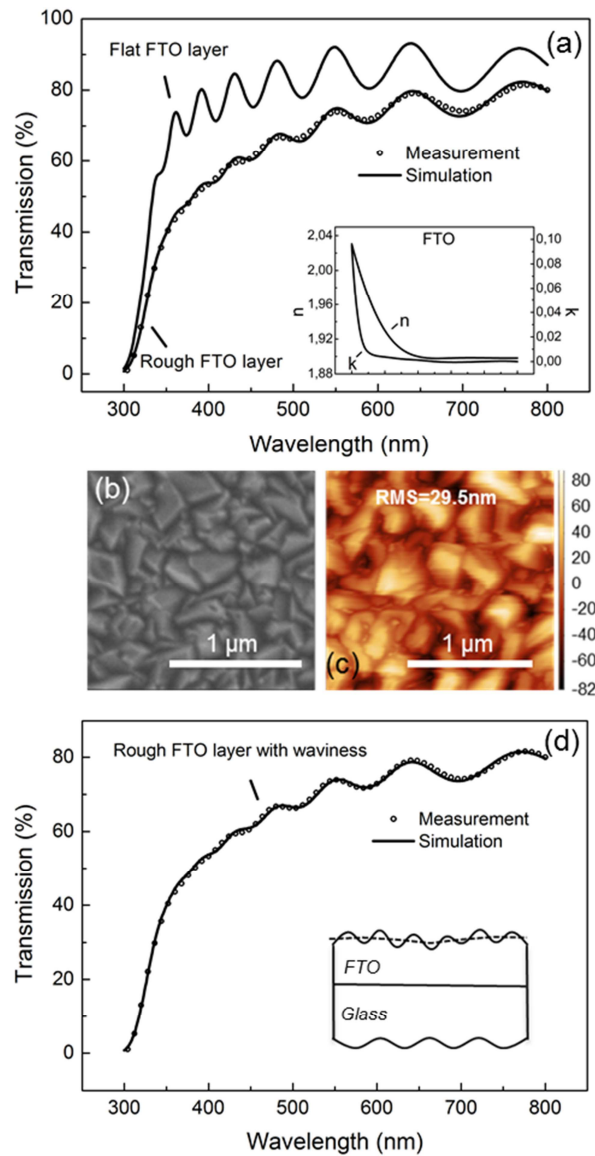


Fig.5. Combined model fitting: (a) Calculated optical transmission curves for the three models: FTO coated substrate plus two effective ZnO layers, FTO layer plus two ZnO effective medium layers with roughness and waviness applied, FTO layer plus a nanosphere layer. The arrows indicate the drop of transmission in the UV and visible range which are respectively the ZnO absorption and light scattering by the nanowires top part. (b) Transmission curve calculated by the combined model (inset image) and corresponding experimental data.

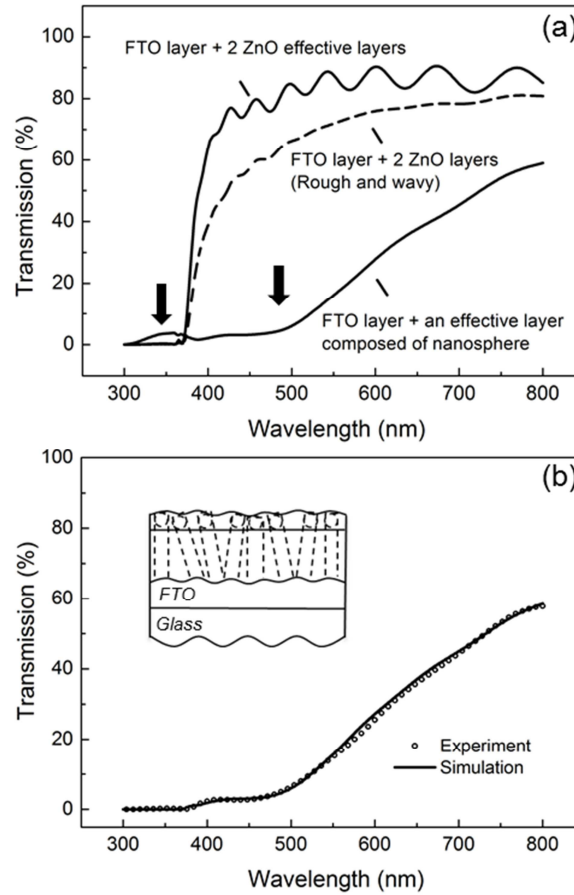




Table 1. Comparison between the measured parameters and the retrieved parameters from the combined model.

Measured parameters	Corresponding retrieved parameters
Thickness of FTO layer: about 1 $\mu\text{m}$	Thickness of FTO layer: 1.01 $\mu\text{m}$
Roughness of FTO layer surface: 29.5 nm (root mean square)	Roughness of FTO layer surface: 29.5 nm (root mean square)
Average diameter of the nanowires: about 200 nm	Diameter of the nanospheres: 220 nm
Average length of the nanowires: about 700 nm	Thickness of effective layer 1: 220 nm Thickness of effective layer 2: 480 nm